Analyzing powers for the $^2H(\vec{p},pn)^1H$ reaction at 200 MeV

W. Pairsuwan,[1,*] J. W. Watson,[1] M. Ahmad,[1,†] N. S. Chant,[2] B. S. Flanders,[1,‡] R. Madey,[1] P. J. Pella,[3] and P. G. Roos[2]
[1]*Department of Physics, Kent State University, Kent, Ohio 44242*
[2]*Department of Physics and Astronomy, University of Maryland, College Park, Maryland 20742*
[3]*Department of Physics, Gettysburg College, Gettysburg, Pennsylvania 17325*
(Received 17 February 1995)

We measured the analyzing power A_y and the triple differential cross section $d^3\sigma/d\Omega_p d\Omega_n dE_p$ for the $^2H(\vec{p},pn)^1H$ reaction at 200 MeV. Coplanar coincidence data were taken for all combinations of neutron angles θ_n=35°, 45°, or 55° with proton angles θ_p=35°, 45°, or 52°. Protons were detected with a ΔE-E telescope with a 1000-μm silicon surface barrier ΔE detector and a plastic scintillator E detector. Neutrons were detected with large-volume plastic scintillators at flight paths of 17.5 or 18 m. The overall neutron separation-energy resolution was about 3 MeV. Data are compared with plane-wave impulse-approximation calculations with a Hulthén deuteron wave function and p-n cross sections and analyzing powers obtained from N-N phase shifts. The agreement between these calculations and the data is generally good for the cross sections. The agreement for the analyzing powers is good near the point of zero recoil momentum. Our results suggest that the deuteron is a good "neutron target" for recoil momenta <100 MeV/c.

PACS number(s): 24.70.+s, 25.10.+s, 25.40.−h

I. INTRODUCTION

The study of spin observables for nuclear reactions has been an active and fruitful area of research in nuclear physics for the past two decades. Data for spin observables generally provide more stringent tests of reaction models than do cross section measurements, because spin observables are sensitive to the details of the reaction dynamics, often isolating interference terms within the reaction amplitude. For projectile energies between 100 and 500 MeV, nuclei are maximally transparent to nucleon projectiles, and single-scattering, impulsive models of reactions are generally applicable. In previous work [1–3] on the $^2H(p,pn)^1H$ reaction, we reported generally good agreement between measured cross sections and plane-wave impulse-approximation (PWIA) calculations. In this paper we extend that work with a systematic study of the analyzing power A_y for this reaction at a beam energy of 200 MeV. We describe the experimental techniques in Sec. II. We describe briefly the PWIA formalism in Sec. III. In Sec. IV we compare the data for both the triple differential cross section $d^3\sigma/d\Omega_p d\Omega_n dE_p$ and the analyzing power A_y with these PWIA calculations. Then we present the summary and conclusions in Sec. V.

II. EXPERIMENTAL TECHNIQUE

We performed this experiment at the Indiana University Cyclotron Facility (IUCF). Figure 1 shows the experimental layout. A 200-MeV beam of polarized protons was incident on a 4.0 ± 0.1 mg/cm^2 deuterated polyethylene (CD_2) target. The beam current ranged between 20 and 60 nA, and the beam polarization was typically 75%. The polarization direction was reversed at the ion source every 60 s. We measured the beam polarization with $p+^4$He elastic scattering with a polarimeter located between the IUCF injector cyclotron and the IUCF main stage cyclotron.

The target chamber and proton telescope for this experiment are shown in Fig. 2. The chamber had a 35 μm thick Kapton window. The movable arm for the proton telescope could be moved in the range 28° ≤ θ_p ≤ 52°. We detected protons with a ΔE-E detector telescope. The ΔE detector was a 1000-μm Si surface barrier detector 50 mm in diameter. The E detector was a 76.2-mm diameter by 127-mm long cylindrical plastic scintillator mounted on a fast photomultiplier tube. A 48-mm thick Pb collimator with a 15.9-mm diameter circular hole collimated the proton flux

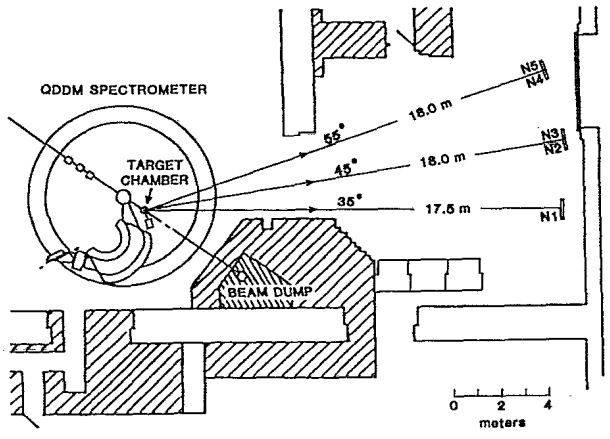

FIG. 1. The experimental area used for the $(\vec{p},pn)$ experiment at the IUCF. The target chamber was located on the beam line for the QDDM spectrometer. $N1$ through $N5$ are the neutron detectors.

*Current address: Fast Neutron Research Facility, Changmai University, Changmai, 50002 Thailand.

†Current address: Faxton Children's Hospital, Radiation Oncology Center, 1676 Sunset Avenue, Utica, NY 13502.

‡Current address: Department of Physics, The American University, Washington, DC 20016.

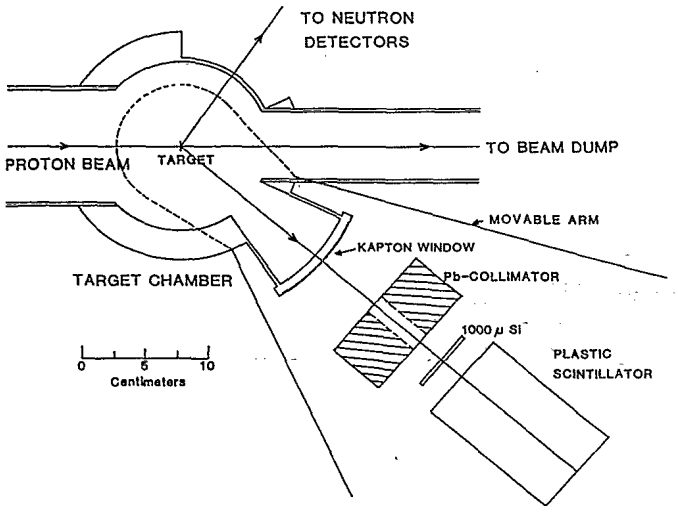

FIG. 2. Experimental configuration of the target chamber and proton detector telescope.

to the proton telescope; the back edge of the collimator was 255.6±2.5 mm from the target yielding a solid angle $\Delta\Omega_p=3.03\pm0.06$ msr. With this proton telescope, we could detect and identify protons with energies between 40 and 136 MeV. The telescope was calibrated with p-p elastic scattering data from a CH_2 target. After matching the gains of the ΔE and E detectors, we used standard particle identification techniques to separate protons from deuterons.

Neutrons were detected with three large-volume, mean-timed neutron detector [4] arrays located at angles θ_n =35°, 45°, and 55° at flight paths of 17.5 m, 18 m, and 18 m, respectively. Each array had a total detector area of 1.02 m ×1.02 m of NE-102 plastic scintillator 0.102 m thick. The neutron solid angles were $\Delta\Omega_n=3.37$ msr for $\Omega_n=35°$ and $\Delta\Omega_n=3.19$ msr for $\theta_n=45°$ and 55°. In front and on top of each neutron detector array we placed a charged particle veto detector to eliminate protons from the target and cosmic ray muons. These detectors were either 9 or 12 mm thick. For each neutron detector array, we measured the veto detector efficiency with protons from p-p elastic scattering from a CH_2 target. The proton telescope was placed at the appropriate angle for p-p elastic scattering; p-p coincidence rates were measured with and without the veto detector in operation. The veto efficiency was found to be greater than 99% for each neutron detector array. These measurements were used also to check the opening angle between the neutron and proton detectors; the measured opening angle was found to be correct to ±0.1°.

We measured neutron times of flight with respect to a signal derived from the cyclotron rf. A train of fast logic pulses was generated from the zero crossing of cyclotron rf signal. A fast timing signal derived from the proton telescope provided a gate to select from this pulse train the appropriate beam pulse to use as the time reference for each event. We utilized the techniques described in Ref. [5] to stabilize the pulse train derived from the cyclotron rf against beam phase drifts. We determined the absolute time-of-flight scale from the time of flight of γ rays from $^{12}C(p,p'\gamma)$ events; a modest number of these events (from the carbon in the CD_2 target) was present in the data we collected.

We established pulse-height calibrations for the neutron detectors using the techniques described in Ref. [4]. Neutron detection efficiencies were calculated with the code of Cecil *et al.* [6]. Pulse height thresholds were typically 10 MeV (electron equivalent) and the corresponding neutron detection efficiencies were between 8% and 11%, depending on the neutron energy.

To measure deadtime losses in the electronics, signals from a multichannel pulser were fed into the electronics to simulate (p,pn) events. These pulser signals had the shape and pulse height to simulate a real neutron-proton coincidence. A peak from the pulser signals appeared in the data in a region removed from the (p,pn) kinematic locus. We estimated deadtime losses from the number of counts in this peak and the number of pulser signals fed into the electronics; deadtime losses were never greater than a few percent.

During data replay, for each event we calculated the energy of the detected proton, E_p, from the proton telescope calibration, and the neutron energy E_n from the known flight path and measured time of flight. We then calculated the neutron separation energy E_s:

$$E_s=E_0-E_p-E_n-(p^2/2M_R) \tag{1}$$

where E_0 is the beam energy (200 MeV), M_R is the mass of the recoil proton, and p is the momentum of the recoil proton derived from the measured energies, known angles, and kinematics.

During data replay we subtracted a random-coincidence sample of data from our measured (p,pn) data. For each angle pair, we generated a spectrum composed solely of random coincidences from the recorded data by analyzing the data with a time origin for the neutron times of flight which was later than the time origin for "real" coincidences by an exact integer number of cyclotron rf periods. This spectrum of random coincidences, taken from a region of unphysical kinematics where neutron times of flight were too short to correspond to real coincidences, was subtracted for the spectrum obtained from analysis with the proper time origin. In the region of the peak cross section for the $^2H(p,pn)^1H$ reaction, these random coincidence spectra were less than 5% of the real (p,pn) data.

Figures 3, 4, and 5 present the final neutron separation energy spectra from this experiment for $\theta_p=35°$, 45°, and 52°, respectively. The peak at 2.2 MeV separation energy is the $p+p+n$ three-body final state. In some spectra a small peak is present around 17 MeV. This is the ground state of ^{11}C from the $^{12}C(p,pn)^{11}C$ reaction on the carbon in the CD_2 target. For $(\theta_p, \theta_n)=(52°, 55°)$ there is so little data for the $^2H(p,pn)$ reaction that we have not included this angle pair in PWIA analysis presented below.

III. PWIA CALCULATIONS

The PWIA is based upon the assumption that the projectile incident on a target nucleus interacts with a single particle inside the nucleus and escapes the nucleus with no further interaction. In other words, the PWIA treats the target nucleus as a perfectly transparent and nonrefracting medium, and the wave functions for the incoming and outgoing particles are approximated as plane waves. At 200 MeV, the

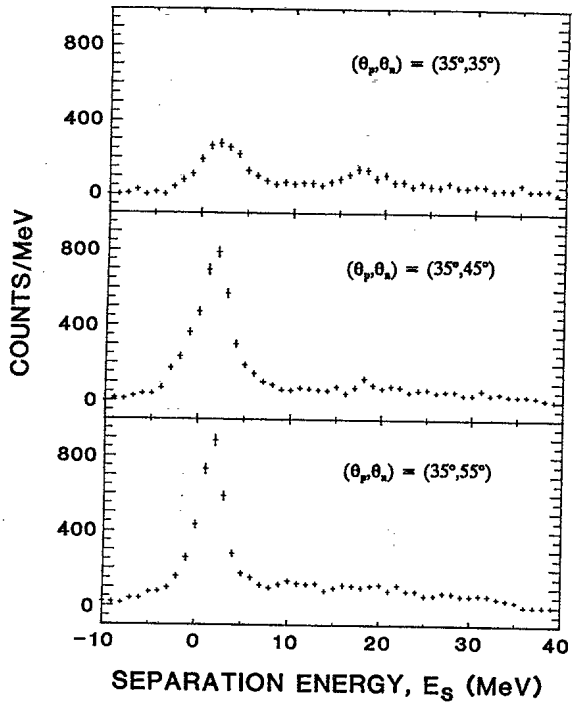

FIG. 3. Separation-energy spectra for the $^2H(\vec{p},pn)$ reaction at 200 MeV with $\theta_p = 35°$ and $\theta_n = 35°$, 45°, and 55°.

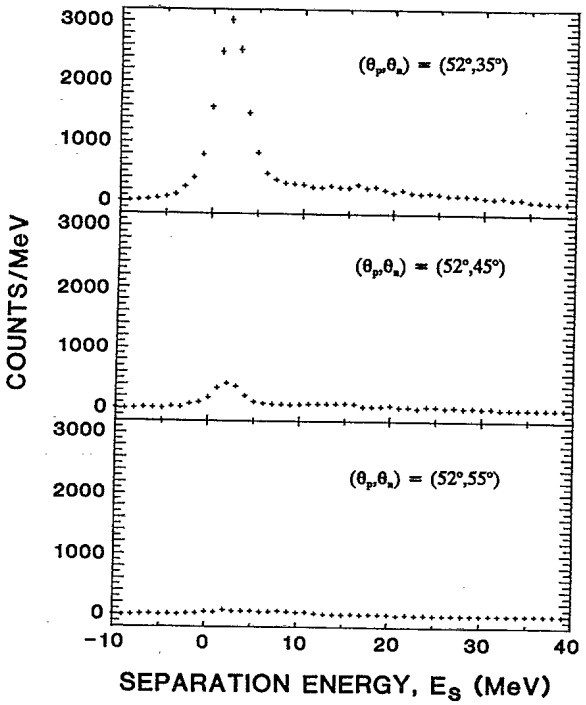

FIG. 5. Separation-energy spectra for the $^2H(\vec{p},pn)$ reaction at 200 MeV with $\theta_p = 52°$ and $\theta_n = 35°$, 45°, and 55°.

$^2H(\vec{p},pn)$ ^1H neutron-knockout reaction on deuterium satisfies this approximation reasonably well. The reduced de Broglie wavelength for the incident proton (~0.3 fm) and the range of the nuclear force (~1.5 fm) are less than the average internucleon spacing (~2.5 fm) in the ^2H nucleus; in addition, the deuteron is a loosely bound nucleus, and multiple scattering effects should be small.

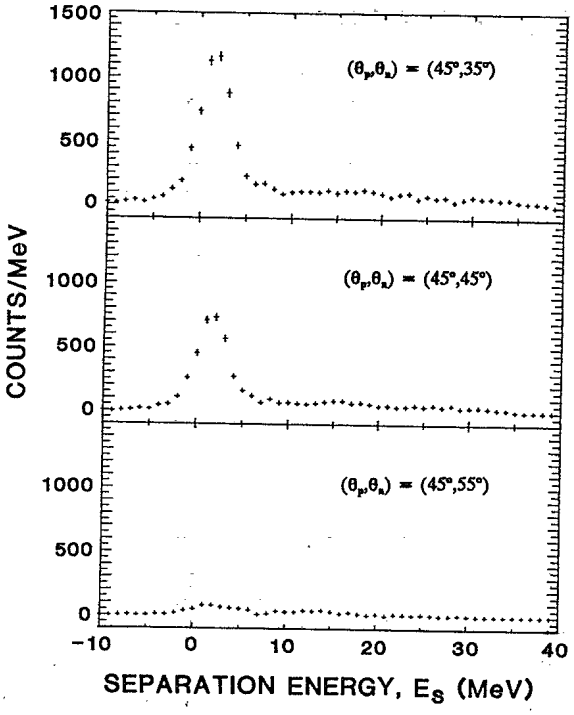

FIG. 4. Separation-energy spectra for the $^2H(\vec{p},pn)$ reaction at 200 MeV with $\theta_p = 45°$ and $\theta_n = 35°$, 45°, and 55°.

Consider an incoming projectile (0) incident on a target (A) resulting in two outgoing particles (1,2) and a residual nucleus (R). In the PWIA, the differential cross section can be written as [7]

$$\frac{d^3\sigma}{d\Omega_1 d\Omega_2 dE_1} = F_{PS}\left(\frac{d\sigma}{d\Omega}\right)_{12} |\phi(p_R)|^2. \tag{2}$$

The factor F_{PS} is a kinematic factor which is proportional to three-body phase space evaluated in a nonrelativistic framework and can be written as

$$F_{PS} = \frac{k_1 k_2}{\hbar^2 k_0}\frac{(m_0+m_2)^2}{m_2}\left[1+\frac{m_2}{m_R}+\frac{m_2 k_1}{m_R k_2}\cos\theta_{12} - \frac{m_2 k_0}{m_R k_2}\cos\theta_2\right]^{-1} \tag{3}$$

where m_0, m_2, and m_R are the masses of 0, 2, and R; k_0, k_1, and k_2 are the wave numbers of particles 0, 1, and 2; and $\theta_{12} = \theta_1 + \theta_2$ is the opening angle between the two detected particles.

The cross section $(d\sigma/d\Omega)_{12}$ is a "half-off-the-mass-shell" two-body cross section evaluated in the center-of-mass of particles 1 and 2; we approximated this cross section according to the prescription of Watson *et al.* [7] by using the free nucleon-nucleon (N-N) cross section at the final-state c.m. energy of particles 1 and 2. The quantity $|\phi(p_R)|^2$ is the probability of finding the neutron with momentum p_R, i.e., $\phi(p_R)$ is the momentum-space wave func-

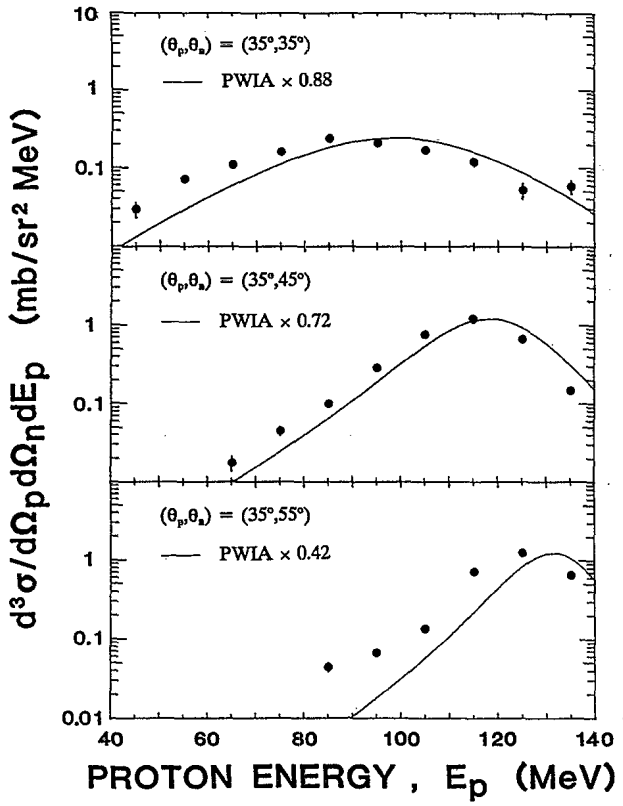

FIG. 6. Triple differential cross sections for the $^2H(\vec{p},pn)$ reaction at 200 MeV with θ_p=35° and θ_n=35°, 45°, and 55°. The solid lines represent the normalized PWIA calculations. The PWIA normalization for each angle pair is shown on the figure.

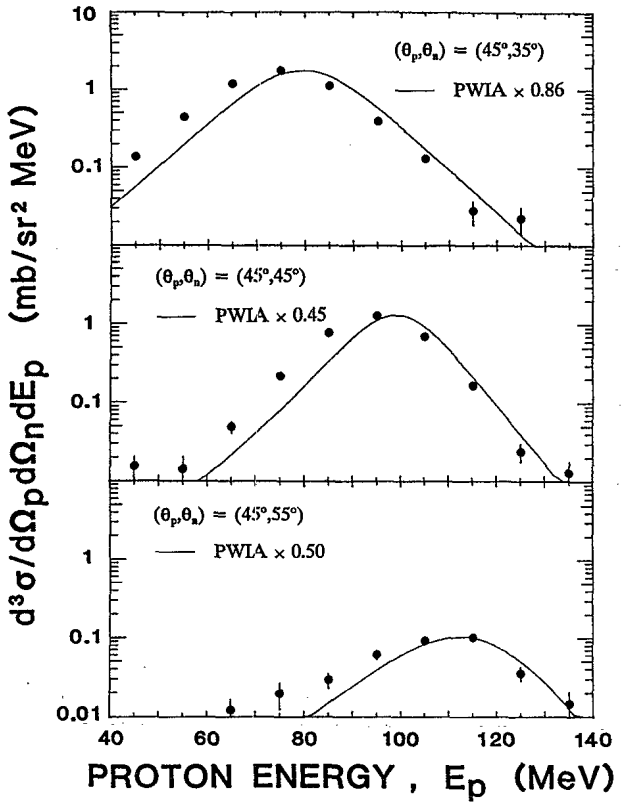

FIG. 7. Triple differential cross sections for the $^2H(\vec{p},pn)$ reaction at 200 MeV with θ_p=45° and θ_n= 35°, 45°, and 55°. The solid lines represent the normalized PWIA calculations. The PWIA normalization for each angle pair is shown on the figure.

tion of the neutron. The PWIA calculations were performed with the code MARILYN described in Ref. [8]. The use of the on-shell approximation with the final-energy prescription is expected to be valid for the $^2H(p,pn)^1H$ reaction especially in the region of small momentum transfers. For deuterium we used a Hulthén momentum wave function of the form [9]

$$\phi(p_R)=\{8\pi\alpha\beta(\alpha+\beta)^3\}^{1/2}\frac{1}{\{\alpha^2+(p_R/\hbar)^2\}\{\beta^2+(p_R/\hbar)^2\}} \quad (4)$$

where α = 0.232 fm^{-1} and β = 1.202 fm^{-1}. Using a wave function with L=0 and L=2 components for the Paris potential changes the PWIA cross sections by less than 5%; the PWIA analyzing powers are independent of the choice of wave function.

IV. COMPARISON OF EXPERIMENT AND PWIA

The triply differential cross sections for the $^2H(\vec{p},pn)$ reaction are shown in Figs. 6, 7, and 8 along with the PWIA calculations generated by the computer code MARILYN. The PWIA calculations were normalized to the data at each angle pair. Although the calculations agree reasonably well with data, the peak in the calculated cross section is shifted to a proton energy approximately 5 MeV higher than the observed peak cross section. This effect appears in a consistent fashion at every angle pair. Although the source of this effect is not clear, it may arise because the PWIA is an oversimplified description of the reaction. Similar shifts were seen in previous studies [1–3] of this reaction at 150 MeV. Note that some of the data for $\theta_p+\theta_n\geq 90°$ show significant final-state

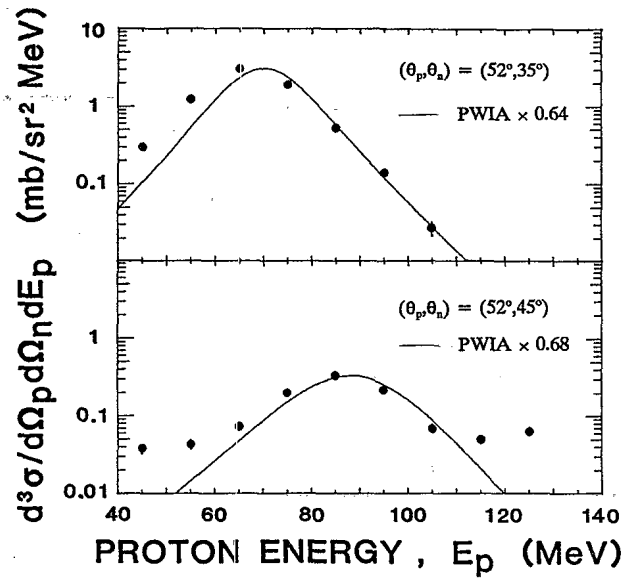

FIG. 8. Triple differential cross sections for the $^2H(\vec{p},pn)$ reaction at 200 MeV with θ_p=52° and θ_n=35° and 45°. The solid lines represent the normalized PWIA calculations. The PWIA normalization for each angle pair is shown on the figure.

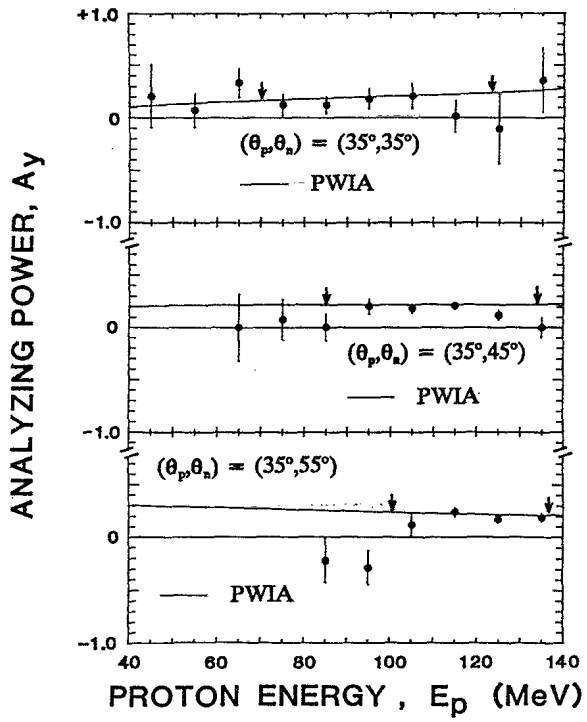

FIG. 9. Analyzing powers for the $^2H(\vec{p},pn)^1H$ reaction at 200 MeV with θ_p=35° and θ_n=35°, 45°, and 55°. The solid lines represent the PWIA calculations. Arrows indicate the small-recoil-momentum region (p_R< 100 MeV/c).

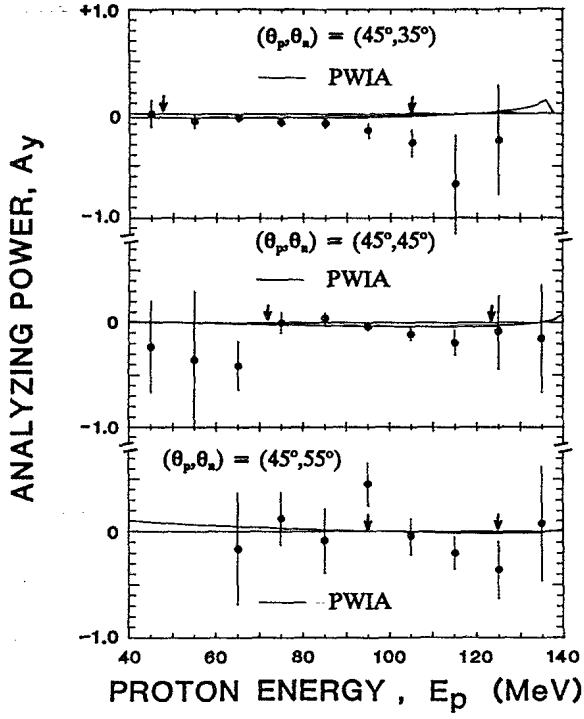

FIG. 10. Analyzing powers for the $^2H(\vec{p},pn)^1H$ reaction at 200 MeV with θ_p=45° and θ_n=35°, 45°, and 55°. The solid lines represent the PWIA calculations. Arrows indicate the small-recoil-momentum region (p_R< 100 MeV/c).

interaction (FSI) contributions well away from the point of minimum recoil momentum, where the PWIA calculations peak. For (θ_p,θ_n)=(45°, 55°) there is significant FSI strength visible for E_p<90 MeV; for (θ_p,θ_n)=(52°, 45°) there is significant FSI strength visible for E_p<60 MeV and E_p>110 MeV.

The observed analyzing powers along with their PWIA comparisons are shown in Figs. 9, 10, and 11. The agreement is reasonably good, especially in the small-recoil-momentum region (p_R<100 MeV/c) where the observed analyzing powers have small statistical uncertainties. The region where p_R<100 MeV/c lies between the arrows in each figure. Above 100 MeV/c, the statistical uncertainties of the observed analyzing powers are large, there can be significant FSI strength which is not described by the PWIA, and the validity of the PWIA may also be questionable.

To show explicitly that the PWIA predictions for analyzing powers work reasonably well in the small-momentum-transfer region, the analyzing powers are plotted for different opening angles ($\theta_p+\theta_n$). Each opening angle corresponds to a different c.m. energy for the N-N collision. The observed analyzing powers at proton energies corresponding to the peak cross section [E_p(peak)] and the PWIA values are plotted in Fig. 12 against the center-of-mass angle of the scattered proton $(\theta_p)_{\text{c.m.}}$ for different opening angles and also are listed in Table I. The agreement between the data and the PWIA is excellent. Clearly, in a situation with minimal distortion, the quasifree analyzing power is described well by the impulse approximation.

An issue of importance in the comparison of the experimental results and the PWIA calculations is the effect of the finite solid angles of the proton and neutron detectors. The PWIA calculations are made for the central angles of the detectors, but the system averages over a range of angles and hence over a range of recoil momenta p_R, the variable used

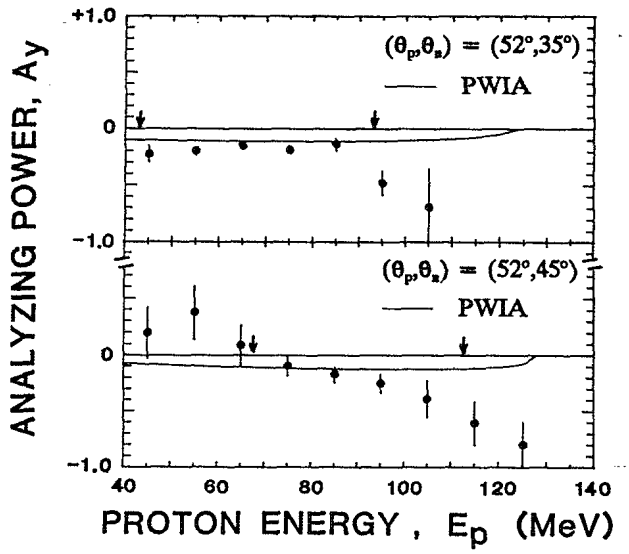

FIG. 11. Analyzing powers for the $^2H(\vec{p},pn)^1H$ reaction at 200 MeV with θ_p=52° and θ_n=35° and 45°. The solid lines represent the PWIA calculations. Arrows indicate the small-recoil-momentum region (p_R< 100 MeV/c).

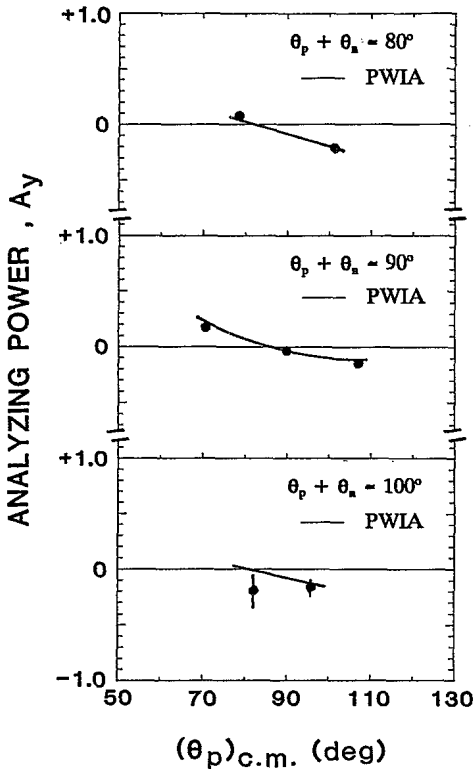

FIG. 12. Analyzing powers for the $^2H(\vec{p},pn)^1H$ reaction at 200 MeV at minimum momentum transfers. The observed analyzing powers at opening angles ($\theta_p+\theta_n$) of about 80°, 90°, and 100° are plotted against the c.m. angles of the scattered proton $(\theta_p)_{c.m.}$. The PWIA calculations are shown as solid lines.

in the ^2H momentum wave function. Typically, the effect of this averaging is important only near the point of minimum p_R in each spectrum where a small reduction in the measured cross section may occur. Monte Carlo simulations suggest that for this experiment the averaging over p_R never reduces the cross section by more than 10%, and that this averaging has no effect on the analyzing powers, which are not sensitive to p_R.

V. SUMMARY AND DISCUSSION

In this paper we reported measurements of the analyzing power A_y for the $^2H(\vec{p},pn)^1H$ reaction at 200 MeV for nine angle pairs. For comparison with these data, we performed PWIA calculations with a Hulthén deuteron wave function and n-p cross sections and analyzing powers calculated from N-N phase shifts.

TABLE I. The observed analyzing powers and the PWIA calculations at E_p(peak) for three sets of opening angles.

(θ_p,θ_n)	$\theta_p+\theta_n$	$(\theta_p)_{c.m.}$	Minimum recoil momentum	Analyzing power, A_y	
(deg)	(deg)	(deg)	q (MeV/c)	PWIA	Observed
35,45	80	78.6	32.7	+0.037	+0.080±0.03
45,35	80	101.5	33.6	−0.217	−0.214±0.04
35,55	90	70.6	27.9	+0.216	+0.170±0.03
45,45	90	89.8	23.3	−0.039	−0.030±0.04
52,35	87	107.0	16.2	−0.114	−0.150±0.02
45,55	100	82.1	81.8	−0.015	−0.194±0.15
52,45	97	95.8	61.9	−0.122	−0.170±0.07

The $^2H(\vec{p},pn)^1H$ data were acquired primarily for testing the analyzing-power prediction of the impulse approximation. In the PWIA, the spin dependence of the nucleon-nucleon interaction alone is responsible for the analyzing power. The experimental $^2H(p,pn)^1H$ cross sections are in fairly good agreement with the PWIA calculations; however, the calculated peak cross section is shifted to proton energies approximately 5 MeV higher than the observed peak cross section for every angle pair. The experimental $^2H(\vec{p},pn)^1H$ analyzing powers in the small-recoil-momentum region (<100 MeV/c) are in good agreement with the PWIA calculations. This suggests that the deuteron may be treated as a "neutron target" if one restricts observations to recoil momenta <100 MeV/c. This is similar to the results reported by Miller *et al.* [10] for the $^3He(\vec{p},pn)$ reaction at 200 MeV with a polarized ^3He target. Miller *et al.* concluded that for momentum transfers to the struck neutron >500 MeV/c, and recoil ("missing") momenta <100 MeV/c, $^3He(\vec{p},pn)$ spin observables are in good agreement with free p-n observables. For the experiment described here on ^2H, the neutron angles $\theta_n \geq 35°$ correspond to momentum transfers ≥370 MeV/c. We also find that for recoil momenta <100 MeV/c A_y for $^2H(\vec{p},pn)$ is in good agreement with A_y for free p-n scattering. It is not surprising that the agreement between $(\vec{p},pn)$ and free p-n spin observables extends to somewhat lower momentum transfers for the ^2H target than for the ^3He target, given the smaller neutron separation energy and larger average internucleon spacing in ^2H.

This research is supported in part by the U.S. National Science Foundation.

[1] J.W. Watson, M. Ahmad, D.W. Devins, B.S. Flanders, D.L. Friesel, N.S. Chant, P.G. Roos, and J. Wastell, Phys. Rev. C **26**, 961 (1982).

[2] Munir Ahmad, J.W. Watson, D.W. Devins, B.S. Flanders, D.L. Friesel, N.S. Chant, P.G. Roos, and J. Wastell, Nucl. Phys. **A424**, 92 (1984).

[3] J.W. Watson, P.J. Pella, M. Ahmad, B.S. Flanders, N.S. Chant, P.G. Roos, D.W. Devins, and D.L. Friesel, J. Phys. (Paris) Colloq. **C4**, 91 (1984).

[4] R. Madey, J.W. Watson, M. Ahmad, B.D. Anderson, A.R. Baldwin, A.L. Casson, W. Cass[illegible], R.A. Cecil, A. Fazely, J.N. Knudson, C. Lebo, W. Pairsuwan, J.C. Varga, and T.R. Witten, Nucl. Instrum. Methods Phys. Res. **214**, 401 (1983).

[5] A.R. Baldwin and R. Madey, Nucl. Instrum. Methods Phys.

Res. **197**, 379 (1982).
[6] R. Cecil, B.D. Anderson, and R. Madey, Nucl. Instrum. Methods **161**, 439 (1979).
[7] J.W. Watson, H.G. Pugh, P.G. Roos, D.A. Goldberg, R.A.J. Riddle, and D.I. Bonbright, Nucl. Phys. **A172**, 513 (1971).
[8] M. Ahmad, Ph.D. dissertation, Kent State University, 1982 (unpublished).
[9] A.F. Kuckes, R. Wilson, and P.F. Cooper, Ann. Phys. (N.Y.) **15**, 193 (1961).
[10] M.A. Miller *et al.*, Phys. Rev. Lett. **74**, 502 (1995).